

# Eulerian modeling and simulation of small scale trajectory crossing and coalescence for moderate-Stokes-number spray flows

By F. Doisneau<sup>†‡</sup>, O. Thomine<sup>¶</sup>, F. Laurent<sup>‡</sup>, A. Vié<sup>‡</sup>, J. Dupays<sup>†</sup>  
AND M. Massot<sup>‡</sup>

A new Eulerian model is derived for polydisperse moderately-inertial sprays with coalescence: an Anisotropic Gaussian Velocity Closure conserves all the second order moments to render the spatial structure of the spray after Droplet Trajectory Crossing. Polydispersity is treated with a high order in size Multi-Fluid method where coalescence terms are directly computed from the velocity reconstructions. The approach is qualified on a crossing jet case against a semi-analytical solution and a Lagrangian Discrete Particle Simulation. The new model is ready for structured grid computations and promising for industrial computations, as it is flexible and of a high order in size and velocity.

---

## 1. Introduction

The accurate simulation of sprays is crucial for industrial applications in mechanical engineering: injection and combustion of liquid fuel in diesel, aeronautical or liquid rocket engines, aluminum oxide residual transport in solid rocket motors, and so on. But simulation raises many issues, such as when droplets are partly driven by their inertia: the liquid disperse phase experiences Droplet Trajectory Crossing (DTC) in the zones of moderate Stokes flows, yielding multiple velocities and eventually coalescing when volume fraction is high enough.

We therefore aim at developing a method that can account for polydispersity, evaporation, and coalescence, as well as strong coupling towards the gas, regardless of the structure of the mean flow and turbulence. Lagrangian approaches easily capture evaporation and crossings but they are difficult to couple to the gas, difficult to parallelize, and costly for unsteady polydisperse sprays (de Chaisemartin 2009; Doisneau *et al.* 2012a), especially coalescence algorithms which are complex to converge (Hylkema & Villedieu 1998). DQMOM approaches have been evaluated to capture the size distribution evolution under coalescence in laminar (Fox *et al.* 2008) and turbulent cases (Belt & Simonin 2009) but they misbehave with evaporation. Finally, Multi-Fluid (MF) methods efficiently capture polydispersity, evaporation (Laurent & Massot 2001) and coalescence (Laurent *et al.* 2004), even in industrial configurations (Doisneau *et al.* 2012b), but they fail when DTC occurs (de Chaisemartin 2009), at least with so-called monokinetic assumptions (Kah *et al.* 2010), as is illustrated for a solid rocket motor nozzle in Doisneau *et al.* (2012a).

We here introduce a new Eulerian model and numerical strategy for polydisperse moderately-inertial particles encountering coalescence: it is a Kinetic Based Moment

<sup>†</sup> Département d'Énergétique Fondamentale et Appliquée (DEFA), ONERA

<sup>‡</sup> Laboratoire EM2C, UPR 288 CNRS and École Centrale Paris

<sup>¶</sup> Institut de Recherche sur la Fusion Magnétique (IRFM), CEA Cadarache

Method (KBMM) with an Anisotropic Gaussian velocity closure (AG) whose parameters are conditioned by size. This closure, also referred to as “10-moment Gaussian” was introduced for rarefied gas dynamics (Levermore & Morokoff 1998), extended and applied to moderate-inertia particle-laden flows in Vié *et al.* (2012*a*) in order to capture local scale DTC, and compared to the so-called Algebraic Closure Based Moment Methods (ACBMM) in Vié *et al.* (2012*b*). We here compute the collision rates directly from the AG velocity closure, allowing to use second order velocity moment information in each direction at crossing locations. The reduction of the formalism regarding the size variable is done with an MF approach based on a Two Size Moment reconstruction that allows us to use few sections and limits the cost from the perspective of industrial computations. We then propose an integration algorithm for the complex velocity integrals arising in the coalescence terms. The extension to evaporation is not discussed but is nevertheless straightforward. The extension to two-way coupling is also relevant, e.g. for solid rocket motors: splitting techniques have been successfully assessed for two-phase acoustics (Doisneau *et al.* 2012*c*) and show promise for the stiff coupling between sections, generated by coalescence, but this is not further discussed here.

The model is implemented in a 2D structured research code; a semi-analytical validation and a comparison to a Lagrangian Discrete Particle Simulation (DPS) are performed on a crossing jet case in order to qualify the proposed approach and assess its potential.

## 2. A Eulerian model for moderately-inertial sprays with coalescence

### 2.1. Kinetic description of sprays

A number density function (NDF)  $f$  describes the spray in a statistical sense, where  $f(t, \mathbf{x}, \mathbf{c}, S) d\mathbf{x} dS d\mathbf{c}$  denotes the average number of droplets at time  $t$ , in a volume of size  $d\mathbf{x}$  around a space location  $\mathbf{x}$ , with a velocity in a  $d\mathbf{c}$ -neighborhood of  $\mathbf{c} = (c_1 \ c_2 \ c_3)^T$  and a surface in a  $dS$ -neighborhood of  $S$ . Since we assume spherical droplets, the relation  $v = \frac{4}{3}\pi r^3 = \frac{1}{6\sqrt{\pi}}S^{\frac{3}{2}}$  between volume  $v$ , surface  $S$ , and radius  $r$  allows the size to be expressed with notations chosen to be most comfortable.

The evolution of the NDF is described by a Boltzmann-like equation (Williams 1958):

$$\partial_t f + \mathbf{c} \cdot \partial_{\mathbf{x}} f + \partial_{\mathbf{c}} \cdot (\mathbf{F} f) = C(f, f) \quad (2.1)$$

where  $\mathbf{F} = (\mathbf{u}_g - \mathbf{c})/\tau_p(S)$  is the drag force per unit mass, here modeled with Stokes’ law for the sake of clarity, with  $\tau_p = \rho_l S/(18\pi\mu_g)$  the particle relaxation time,  $\mathbf{u}_g(t, \mathbf{x})$  the local gas velocity,  $\mu_g$  its dynamic viscosity, and  $\rho_l$  the liquid density. We consider coalescence between droplets, through the source term  $C$ , modeled at the kinetic level (Hylkema & Villedieu 1998) with the assumptions of Laurent *et al.* (2004):

[HC1] We only take binary collisions into account.

[HC2] The mean collision time is very small compared to the intercollision time.

[HC3] Mass and momentum are preserved during collisions.

[HC4] Every collision leads to coalescence.

Hypotheses [HC1] and [HC2] result from the small liquid phase volume fraction in the context of moderately dense sprays. Hypothesis [HC4] is taken for the sake of clarity but rebounds and separation, by reflexion or stretching, can be treated as discussed in Hylkema & Villedieu (1998) and references therein. Considering two precursor droplets of volumes  $v^*$  and  $v^\diamond$  colliding to form a new droplet of volume  $v$ , the kinetic coalescence

operator reads (Hylkema & Villedieu 1998):

$$\begin{aligned} \mathbf{C} = & \frac{1}{2} \int_{\mathbf{c}^* \in \mathbb{R}^{N_d}} \int_{v^* \in [0, v]} f(t, \mathbf{x}, \mathbf{c}^*; v^*) f(t, \mathbf{x}, \mathbf{c}^\diamond; v^\diamond) \mathfrak{B}(v^*, v^\diamond; \mathbf{c}^*, \mathbf{c}^\diamond) J dv^* d\mathbf{c}^* \\ & - \int_{\mathbf{c}^* \in \mathbb{R}^{N_d}} \int_{v^* \in [0, +\infty[} f(t, \mathbf{x}, \mathbf{c}, v) f(t, \mathbf{x}, \mathbf{c}^*; v^*) \mathfrak{B}(v, v^*; \mathbf{c}, \mathbf{c}^*) dv^* d\mathbf{c}^* \end{aligned} \quad (2.2)$$

where  $\mathfrak{B}$  is the collision/coalescence probability kernel,  $N_d$  is the dimension of the velocity phase space and  $J = (v/v^\diamond)^{N_d+1}$  is the Jacobian of the mapping  $(v, \mathbf{c}) \rightarrow (v^\diamond, \mathbf{c}^\diamond)$ . The physics of coalescence at the microscopic (droplet) level is rendered through the choice of the  $\diamond$  state with respect to:

$$\begin{cases} v = v^* + v^\diamond & \text{mass conservation with constant } \rho_l \text{ density} \\ v\mathbf{c} = v^*\mathbf{c}^* + v^\diamond\mathbf{c}^\diamond & \text{momentum conservation} \\ (v\mathbf{c})^2 = (v^*\mathbf{c}^* + v^\diamond\mathbf{c}^\diamond)^2 & \text{kinetic energy loss for perfectly inelastic collision} \end{cases} \quad (2.3)$$

The kernel  $\mathfrak{B}(v^*, v^\diamond; \mathbf{c}^*, \mathbf{c}^\diamond) = \pi (r^* + r^\diamond)^2 |\mathbf{c}^\diamond - \mathbf{c}^*| \triangleq \beta^s(v^*, v^\diamond) \beta^u(\mathbf{c}^*, \mathbf{c}^\diamond)$  is factorized in a size-dependent kernel called geometric cross-section and a velocity-dependent kernel, here a kinetic velocity difference. Note that  $\beta^s(v^*, v^\diamond) = r^* + r^\diamond$  in 2D, i.e., when all the initial centers of mass and velocity vectors belong to the same plane.

## 2.2. Gaussian closure at the semi kinetic level

To reduce the size of the phase space, we assume the following NDF form (Levermore & Morokoff 1998; Vié *et al.* 2012a):

$$[\text{HV1}] \quad f(t, \mathbf{x}, \mathbf{c}, S) = n(t, \mathbf{x}, S) \mathcal{N}(\mathbf{c}; \mathbf{u}(t, \mathbf{x}, S), \mathbf{\Sigma}(t, \mathbf{x}, S)) \quad (2.4)$$

where  $\mathcal{N}$  is a joint Gaussian distribution with  $\mathbf{u} = (u_1 \ u_2 \ u_3)^T$  its center and  $\mathbf{\Sigma} = (\sigma_{ij})$  its  $3 \times 3$  covariance matrix, taken symmetric:

$$\mathcal{N}(\mathbf{c}; \mathbf{u}, \mathbf{\Sigma}) = \frac{\det(\mathbf{\Sigma})^{-\frac{1}{2}}}{(2\pi)^{\frac{1}{2}N_d}} \exp\left(-\frac{1}{2}(\mathbf{c} - \mathbf{u})^T \mathbf{\Sigma}^{-1}(\mathbf{c} - \mathbf{u})\right).$$

The covariance matrix must respect some realizability conditions that are the strict positivity of the diagonal coefficients  $\sigma_{ii}$  and of  $\det(\mathbf{\Sigma})$ , in link with entropies. Both average  $\mathbf{u}(t, \mathbf{x}, S)$  and dispersion  $\mathbf{\Sigma}(t, \mathbf{x}, S)$  are conditioned by size. We then need to solve for ten velocity moments in 3D. For the sake of clarity, we now detail the method in 2D so we need only six moments  $\mathcal{M} = (n \ nu_1 \ nu_2 \ n(u_1^2 + \sigma_{11}) \ n(u_1 u_2 + \sigma_{12}) \ n(u_2^2 + \sigma_{22}))^T$  which are generated by the vector of velocity polynomials  $\mathcal{M}^u(\mathbf{c}) = (1 \ c_1 \ c_2 \ c_1^2 \ c_1 c_2 \ c_2^2)^T$ . After integration of the kinetic equation (2.1) with respect to the kinetic velocity variable  $\mathbf{c}$ , we get the system of conservation equations with source terms:

$$\partial_t \mathcal{M} + \partial_{\mathbf{x}} \cdot \mathcal{F}(\mathcal{M}) = \mathcal{S}(\mathcal{M}) + \mathcal{C}(\mathcal{M}, \mathcal{M}) \quad (2.5)$$

where the flux vector  $\mathcal{F} = (\mathcal{F}_1 \ \mathcal{F}_2)^T$  depends on unresolved, third order moments that can be computed from  $\mathbf{u}$  and  $\mathbf{\Sigma}$  thanks to the Gaussian profile and where the source term vector  $\mathcal{S}$  depends on known moments. They read:

$$\mathcal{F}_1 = n \begin{pmatrix} u_1 \\ u_1^2 + \sigma_{11} \\ u_1 u_2 + \sigma_{12} \\ u_1^3 + 3u_1 \sigma_{11} \\ u_1^2 u_2 + 2u_1 \sigma_{12} + u_2 \sigma_{11} \\ u_1 u_2^2 + u_1 \sigma_{22} + 2u_2 \sigma_{12} \end{pmatrix}, \quad \mathcal{S} = \frac{n}{\tau^{\mathbf{u}}} \begin{pmatrix} 0 \\ -u_1 + u_{g,1} \\ -u_2 + u_{g,2} \\ -2\sigma_{11} - 2u_1^2 + u_1 u_{g,1} \\ -2\sigma_{12} - 2u_1 u_2 \\ -2\sigma_{22} - 2u_2^2 + u_2 u_{g,2} \end{pmatrix}$$

where  $\mathcal{F}_2$  is deduced by obvious substitutions. The coalescence operator integrates as:

$$\begin{aligned} \mathcal{C} = & \frac{1}{2} \iint_{\mathbb{R}^{2N_d}} \int_{v^* \in [0, v]} \mathcal{C}(\mathbf{c}^*, \mathbf{c}^\diamond) n(v^*) \mathcal{N}(\mathbf{c}^*; v^*) n(v^\diamond) \mathcal{N}(\mathbf{c}^\diamond; v^\diamond) \mathfrak{B}(v^*, v^\diamond; \mathbf{c}^*, \mathbf{c}^\diamond) dv^* d\mathbf{c}^* d\mathbf{c}^\diamond \\ & - n(v) \iint_{\mathbb{R}^{2N_d}} \int_{v^* \in [0, +\infty[} \mathcal{M}^u(\mathbf{c}) \mathcal{N}(\mathbf{c}; v) n(v^*) \mathcal{N}(\mathbf{c}^*; v^*) \mathfrak{B}(v, v^*; \mathbf{c}, \mathbf{c}^*) dv^* d\mathbf{c}^* d\mathbf{c} \end{aligned} \quad (2.6)$$

where the velocity distributions are conditioned by size through their macroscopic parameters, e.g.  $\mathcal{N}(\mathbf{c}^*; v^*) = \mathcal{N}(\mathbf{c}^*; \mathbf{u}(v^*), \boldsymbol{\Sigma}(v^*))$  and where  $\mathcal{C}$  is the coalescence creation function vector, that renders the transformations of coalescence on microscopic variables from relations (2.3). The latter reads, keeping in mind that  $v = v^* + v^\diamond$ :

$$\mathcal{C}(\mathbf{c}^*, \mathbf{c}^\diamond) = \begin{pmatrix} 1 \\ (v^* c_1^* + v^\diamond c_1^\diamond)/v \\ (v^* c_2^* + v^\diamond c_2^\diamond)/v \\ (v^* c_1^* + v^\diamond c_1^\diamond)^2/v^2 \\ (v^* c_1^* + v^\diamond c_1^\diamond)(v^* c_2^* + v^\diamond c_2^\diamond)/v^2 \\ (v^* c_2^* + v^\diamond c_2^\diamond)^2/v^2 \end{pmatrix}. \quad (2.7)$$

The above vector can be decomposed, in the present modeling, as a vector  $\mathfrak{P}$  of linear combinations of size monomials  $\mathcal{C}^s(v^*, v^\diamond) = (1 \ v^*/v \ v^\diamond/v \ v^{*2}/v^2 \ v^* v^\diamond/v^2 \ v^{\diamond 2}/v^2)^T$  and second order velocity monomials  $\mathcal{C}^u(\mathbf{c}^*, \mathbf{c}^\diamond) = (1 \ \mathbf{c}_1^* \ \mathbf{c}_1^\diamond \ \mathbf{c}_2^* \ \mathbf{c}_2^\diamond \ \mathbf{c}_1^{*2} \ \mathbf{c}_1^{\diamond 2} \ \mathbf{c}_1^* \mathbf{c}_1^\diamond \ \mathbf{c}_2^* \mathbf{c}_2^\diamond \ \mathbf{c}_1^* \mathbf{c}_2^\diamond \ \mathbf{c}_2^* \mathbf{c}_1^\diamond)^T$ . This decomposition formally reads  $\mathcal{C}(\mathbf{c}^*, \mathbf{c}^\diamond) \triangleq \mathfrak{P}(\mathcal{C}^s(v^*, v^\diamond), \mathcal{C}^u(\mathbf{c}^*, \mathbf{c}^\diamond))$  and allows to compute separately velocity and size integrals in the following.

### 2.3. Multi-Fluid approach with the Anisotropic Gaussian velocity closure

The second modeling step leads to the so-called Eulerian Multi-Fluid model (Laurent & Massot 2001), here applied to the previous semi-kinetic approach with AG. We choose a discretization  $0 = S_0 < S_1 < \dots < S_{N_{\text{sec}}} = +\infty$  for the droplet size phase space and we average system (2.5) over each fixed size interval  $\mathcal{S}_k = [S_{k-1}, S_k[$ , called section. The set of droplets in one section can be seen as a “fluid” for which conservation equations are written, the sections exchanging mass, momentum and enthalpy. In order to close the system, assumptions are introduced in each section  $k$ :

[HS1] The form of  $n(S) = \kappa_k^s(S)$  is presumed.

[HV2] The form of  $\mathcal{N}$  is fixed as  $\mathcal{N}_k$  so that  $(\mathbf{u}(S), \boldsymbol{\Sigma}(S)) = (\mathbf{u}_k, \boldsymbol{\Sigma}_k)$ .

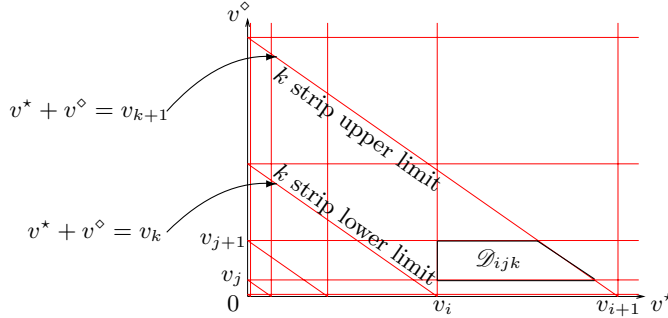
We consider a Two Size Moment approach which is described in Doisneau *et al.* (2012b) so the distributions chosen for [HS1] have two parameters and the two corresponding moments are number  $n_k$  and mass  $m_k$ , generated by integration versus  $\mathcal{M}_k^s(S) = (1 \ \frac{\rho_l S^{\frac{3}{2}}}{6\sqrt{\pi}})^T$  on  $\mathcal{S}_k$ . After integration of (2.5) on the  $\mathcal{S}_k$ , we get the Multi-Fluid systems:

$$\partial_t \mathcal{M}_k + \partial_{\mathbf{x}} \cdot \mathcal{F}_k(\mathcal{M}_k) = \mathcal{S}_k(\mathcal{M}_k) + \mathcal{C}_k((\mathcal{M}_i)_{1, N_{\text{sec}}}) \quad (2.8)$$

on  $\mathcal{M}_k = (n_k \ m_k \ m_k u_{k1} \ m_k u_{k2} \ m_k (u_{k1}^2 + \sigma_{k11}) \ m_k (u_{k1} u_{k2} + \sigma_{k12}) \ m_k (u_{k2}^2 + \sigma_{k22}))^T$ , vectors of the variables of section  $k$ , which have seven (eleven) elements in 2D (3D). The coalescence terms are now size and velocity integrals, decomposed as sums thanks to the continuity of the size partitioning in sections:

$$\mathcal{C}_k((\mathcal{M}_i)_{i=1, N_{\text{sec}}}) = \sum_{i+j=k} \mathfrak{P}_{\text{MF}}(\mathcal{I}_{ij}^u, \mathcal{I}_{ijk}^s) - \sum_{i,j} \mathfrak{P}_{\text{MF}}(\mathcal{I}_{ki}^u, \mathcal{I}_{kij}^s) \quad (2.9)$$

where the two terms have been integrated in the context of the creation terms, the disappearance terms being recombined to ensure mass conservation. We highlight that

FIGURE 1. Domains  $\mathcal{D}_{ijk}$  on which coalescence terms are size-integrated.

$\mathfrak{P}_{\text{MF}}$  is still a vector of linear combinations of size and velocity monomials but with respect to the required size moments at the Multi-Fluid level. The velocity integrals:

$$\mathcal{I}_{ij}^u = \iint_{(\mathbf{c}^*, \mathbf{c}^\diamond) \in \mathbb{R}^{2N_d}} \mathcal{C}^u(\mathbf{c}^*, \mathbf{c}^\diamond) \mathcal{N}_i(\mathbf{c}^*) \mathcal{N}_j(\mathbf{c}^\diamond) \beta^u(\mathbf{c}^*, \mathbf{c}^\diamond) d\mathbf{c}^* d\mathbf{c}^\diamond \quad (2.10)$$

have been integrated twice on the velocity phase space, and the size integrals:

$$\mathcal{I}_{ijk}^s = \iint_{(S^*, S^\diamond) \in \mathcal{D}_{ijk}} \mathcal{C}_{\text{MF}}^s(S^*, S^\diamond) \kappa_i^s(S^*) \kappa_j^s(S^\diamond) \beta^s(S^*, S^\diamond) dS^* dS^\diamond \quad (2.11)$$

have been integrated on a section and on a portion of the partner size space. Yet the first dependency does not coincide with any section after mapping onto the colliding partners  $i$  and  $j$ . So domains are defined to ensure mass conservation (Laurent *et al.* 2004; Doisneau *et al.* 2012b) as illustrated in Figure 1 and they are triply indexed with the two precursor section numbers  $i$  and  $j$  and the destination section number  $k$ .

#### 2.4. Numerical approach of coalescence velocity integrals

Since the velocity reconstruction  $\mathcal{N}_k(\mathbf{c}; \mathbf{u}_k, \Sigma_k)$  and size reconstruction  $\kappa_k^s(S)$  change at each time and location, we need to compute the coalescence integrals very often and for each pair of sections. The size integrals (2.11) on  $\mathcal{D}_{ijk}$  are complex as usual in MF so we use an adaptive quadrature method that was developed in Doisneau *et al.* (2012b). But the velocity integrals (2.10) here require four-dimensional integrations and even six-dimensional integrations in 3D while monokinetic MF needed trivial integrations on Dirac delta functions. We therefore choose a Gauss-Hermite quadrature, which avoids computing the exponential kernel at the nodes. The use of 4 nodes yields an acceptable maximum error of 10% on the velocity integrals. We highlight that using fewer nodes generates unacceptable errors because of the norm function in the integrand, which is non-smooth.

### 3. Lagrangian approach: a reference

The Lagrangian DPS approach, introduced by Dukowicz (1980), is a deterministic resolution of a particulate problem, therefore not based on Eq. (2.1). In this approach, each particle  $i$  among  $N_p$  corresponds to a physical particle transported thanks to the ordinary differential equations of its center of mass position  $\mathbf{x}_i$  and velocity  $\mathbf{u}_i$ :

$$\partial_t \mathbf{x}_i = \mathbf{u}_i; \quad \partial_t \mathbf{u}_i = \mathbf{F}_i \quad (3.1)$$

while coalescence is rendered deterministically with a collision detection algorithm, each collision producing a unique particle out of two, according to the transformations (2.3).

We briefly describe the algorithm presently used and refer to Thomine (2011) for further details. Transport is divided in time steps, which need to be small enough to avoid more than one collision per particle. The collision detection algorithm determines for each particle if the particles in a neighborhood are to collide. The neighborhood is chosen to reduce the cost of the algorithm significantly below the theoretical limit  $N_p(N_p - 1)$ . The DPS algorithm decomposes on a time step as follows:

- (a) collision detection;
- (b) time resolution of Eq. (3.1) with a 3rd order Runge-Kutta method;
- (c) position and velocity update for colliding particles.

The direct comparison between such a deterministic approach and a Eulerian statistical approach, especially when particle interactions are present or for unsteady turbulent flows, may lead to serious difficulties. Ensemble-averaging on many DPS realizations, using random initial and boundary conditions, is generally needed. However, in statistically steady configurations, such as the one chosen below, time-averaging one DPS realization and considering the steady state of the Eulerian simulation yield comparable quantities.

#### 4. Case of two jets crossing with a co-flow

##### 4.1. General characteristics of a coalescing crossflow

We consider a 2D case of two jets injected at a velocity  $(u_0, \pm v_0)$  whose trajectories cross because of the droplet inertia before being bent by a gaseous co-flow of velocity  $(u_0, 0)$ . The spray is here characterized by two non-dimensionalized numbers:

- a Stokes number that determines the curvature of each jet and the way they cross;
- a Knudsen number that gives the intensity of collisions and therefore coalescence.

The Stokes number is defined as the ratio  $St = \tau_0^u / \tau_m$  where  $\tau_0^u$  is the Stokes time associated to the injected particles and  $\tau_m = \eta_0 / v_0$  is the time required for a particle to meet the centerline at constant velocity  $v_0$  from an initial distance of the centerline  $\eta_0$ . Noticeably, a finite inertia droplet encountering Stokes drag travels exactly a distance  $\tau_0^u v_0$  in the vertical direction before stopping so that:

$$St = \frac{\tau_0^u v_0}{\eta_0} \quad (4.1)$$

is a ratio of lengths and droplets with  $St > 1$  are the only one to cross the centerline. We then define a coalescing Knudsen number  $Kn_{\text{coal}} = (\nu_{\text{coal}} \tau_{ol})^{-1}$  to quantify the intensity of coalescence (Doisneau *et al.* 2012b) where  $\nu_{\text{coal}}$  is a coalescence frequency and  $\tau_{ol}$  is a flow characteristic time, here the time during which the two jet footprints overlap. In a crossflow that is initially monodisperse, it reads:

$$Kn_{\text{coal}} = \frac{\rho_l r_0 |\mathbf{u}_0|}{12 m_0 v_0 d_0} \quad (4.2)$$

where the initial state is described by  $r_0$  the droplet radius,  $\rho_0$  the initial mass concentration,  $d_0$  the width of each jet and  $|\mathbf{u}_0|$  the injection velocity norm.

We now set  $u_0 = 10\text{m/s}$  for the gas to flow permanently from left to right. The injection conditions are: two jets wide of  $d_0 = 0.01\text{m}$  and separated by  $2\eta_0 = 0.1\text{m}$ , of monodisperse particles with  $r_0 = 18\mu\text{m}$  injected at  $u_0 = 10\text{m/s}$  and  $|v_0| = 10\text{m/s}$ . We set the gas viscosity  $\mu_g$  and the liquid density  $\rho_l$  to have  $\tau_0^u = 7.5\text{ms}$  and  $St = 1.5$  so that the two jets cross. Because of the initial monodisperse condition, coalescence yields size modes, i.e., droplets, with an integer multiple  $k\mathcal{V}(r_0)$  of the initial droplet volume  $\mathcal{V}(r_0)$  so the size distribution is discrete. We here choose an MF discretization for each mode

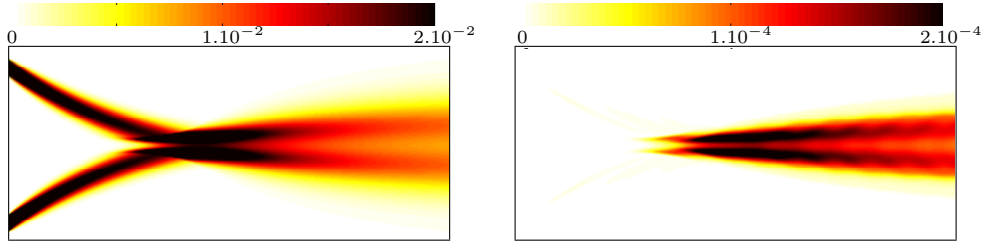


FIGURE 2. Mass concentration ( $\text{kg}/\text{m}^3$ ) for  $\text{Kn}_{\text{coal}} = 100$  with Eulerian approach (SAP2) – Left: Section 1 (mode 0); Right: Section 2 (mode 1).

to match exactly one section, e.g., its right bound  $\mathcal{V}(S_k) = k\mathcal{V}(r_0)$ . As for coalescence intensity, we consider two cases with different  $\text{Kn}_{\text{coal}}$  by setting two different injection concentrations  $m_0$ : a high Knudsen case which is weakly coalescing and can be linearized and a low Knudsen case which is more complex. To perform these two cases, the new Eulerian model is implemented in a research code called SAP2 and run on a 2D  $256^2$  grid with 8 sections.

#### 4.2. Weakly coalescing case

The first practical case has an initial particle concentration in each jet that yields  $\text{Kn}_{\text{coal}} \gg 1$ . So coalescence is weak and very few new droplets are created. The coalescence terms are then linearized by neglecting (i) the mass taken from the initial section, and (ii) the interactions between two non-initial sections. This gives immediately a semi-analytical estimation of the droplets produced at the exit of the crossing as proportional to  $\text{Kn}_{\text{coal}}$ . So the formula reads for the section concentrations after the crossing, thanks to the mode/section equivalence:

$$m_{k+1} = \frac{1}{\text{Kn}_{\text{coal}}} m_k. \quad (4.3)$$

This relation is written indifferently in total mass or mass concentration thanks to the sufficient homogeneity of the problem. A case with  $\text{Kn}_{\text{coal}} = 100$  is admissible as weakly coalescing. In this regime, a small mass concentration of droplets of mode 1 ( $r_1 = 22.7\mu\text{m}$ ) appears at the right edge of section 2, and even smaller amounts of the following modes appear in the following sections according to (4.3).

On the one hand, we examine the overall dynamics of the problem. First, we consider the infinite Knudsen, i.e. non colliding case, as a reference: its trajectories can be computed analytically as exponentials. Second, we compare it to the infinite Knudsen case with any AG based Eulerian method: most of the mass is enclosed in the analytical trajectories so the spatial repartition is well reproduced, at least regarding the size of the jet characteristic structures thanks to AG (Vié *et al.* 2012a). Third, we compare the results with finite Knudsen and coalescence given in Figure 2: they match the infinite Knudsen Eulerian results, which is relevant since coalescence is too weak to disturb the spray dynamics. So the spray dynamics is well rendered by the new model.

On the other hand, we examine size growth under coalescence: Figure 2 shows that the Eulerian mass concentrations in section 2 after the crossing are a hundred times, i.e. about  $\text{Kn}_{\text{coal}}$  times, below the ones in section 1. This matches the semi-analytical estimation (4.3) so we get a quantitative validation of the approach for the linearized case. As a conclusion for this crossing jet, spray dynamics is well rendered and coalescence intensity is quantitatively captured by the new Eulerian model.

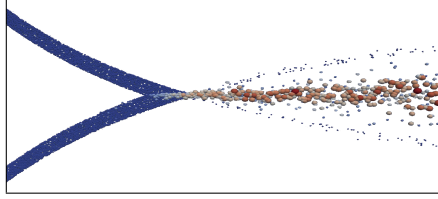


FIGURE 3. Instantaneous location of particles colored by size for  $\text{Kn}_{\text{coal}} = 1$  with Lagrangian approach (Asphodele).

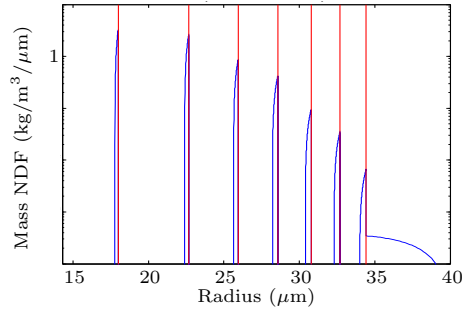


FIGURE 4. Mass density function (log-scale) at the output on centerline for  $\text{Kn}_{\text{coal}} = 1$  with Eulerian approach (SAP2).

#### 4.3. Non-linear case

We now take  $\text{Kn}_{\text{coal}} = 1$ . So a significant portion of the droplets encounter coalescence and change size: all droplet modes can significantly interact with themselves and the others so the problem is non-linear and complex. A reference solution is computed with the Asphodele code (Reveillon & Demoulin 2007; Thomine 2011), using a Lagrangian DPS approach to account for such complexity. The Lagrangian solution has a very complex dynamics, as illustrated on an instantaneous realization in Figure 3. We give in Figure 5 the mass repartition for the different sections with the new Eulerian approach.

First, we observe that the jet spreads less after the crossing point than for cases with higher Knudsen. Since coalescence corresponds to a perfectly inelastic collision, which destroys the relative kinetic energy of the two jets, the jet angle after crossing is reduced contrary to rebounds which would redistribute kinetic energies and widen the jet angle. In particular, we observe in Figure 5 the Eulerian mass repartition of the different sections getting closer to the centerline as the mode number increases. This matches the trend of coalescence to destroy relative kinetic energy since higher sections, i.e., modes have encountered more coalescence. So the jet angle gives quantitative information about the correct treatment of coalescence by the method. We extrapolate that in the case of  $\text{Kn} = 0$ , we get a  $\delta$ -shock on the centerline. In the present case of  $\text{Kn} = 1$  the Eulerian jet angle compares well to the Lagrangian reference case.

Second, the Eulerian size distribution at the jet output that is given in Figure 4 proves that the modes of coalescence are very well captured, the size distribution remaining steep despite a slight numerical diffusion in size phase space. The size discretization has of course been chosen for each mode (up to nine) to match a section, but the two-size moment approach is known to deal efficiently with complex size distributions with a low number of sections. This feature is desired for advanced or industrial computations (Doisneau *et al.* 2012b) and we here show the ability of the new model to do so.

Third, we observe in Figure 6 the average  $d_{30}$  diameter, as computed with both approaches. The droplet size repartition is well rendered with the Eulerian approach, with the bigger, less agitated droplets on the centerline, and small droplets, which avoided coalescence events, more on the sides. So the complex dynamics of coalescence at a crossing location is captured by the new Eulerian model.

To conclude on the crossing jet case the configuration appears to have a very complex physics, which can be captured exactly only with a Lagrangian DPS -if that, not for numerous particle cases. But the new Eulerian model renders quantitatively the main features that are size growth, size repartition and jet angle, these quantities being suf-

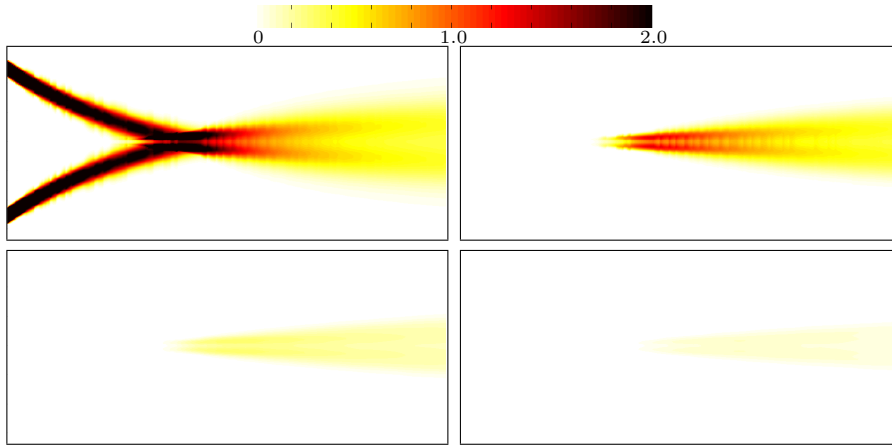


FIGURE 5. Mass concentration per section with Eulerian approach (SAP2) – Top left to bottom right: section 1 to 4

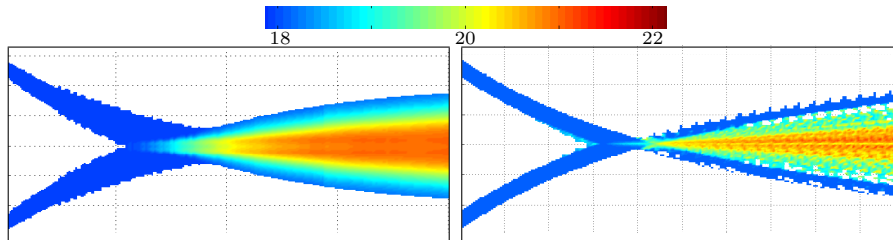


FIGURE 6. Volume average radius  $r_{30}$  ( $\mu\text{m}$ ) of the overall distribution – Left: Eulerian (SAP2); Right: Time average Lagrangian (Asphodele).

ficient for industrial applications. In solid rocket motors, for instance, computing the disperse phase retroaction on the flow in the nozzle requires a rough knowledge of the droplet jet inertia and angle after crossing. Moreover, the variety of sizes and trajectories that arises in industrial cases, featuring turbulent flows and many crossings, make Lagrangian simulations intractable while Eulerian models can approach the dynamics.

## 5. Conclusion

The new Eulerian model, based on the Anisotropic Gaussian velocity closure and the Two Size Moment Multi-Fluid method, captures the main features of spreading and coalescence growth when Droplet Trajectory Crossing occurs. This makes it suitable for capturing the dynamics of polydisperse moderately-inertial spray flows with coalescence, especially when such flows become complex, excluding Lagrangian approaches. The approach is valid for structured grid computations and promising for industrial computations thanks to the Two Size Moment method, which allows limiting the number of sections and the cost.

### *Acknowledgments*

The present research was sponsored by an ONERA grant in the context of PEA Nano2 (J. Dupays). The support of the France-Stanford Center for Interdisciplinary Studies through a collaborative project grant (P. Moin/M. Massot) is gratefully acknowledged. The authors also acknowledge CTR for their hospitality and their financial support.

## REFERENCES

- BELT, R. & SIMONIN, O. 2009 Quadrature method of moments for the pdf modeling of droplet coalescence in turbulent two-phase flow. *ASME Conference Proceedings* **2009** (78095), 783–793.
- DE CHAISEMARTIN, S. 2009 Polydisperse evaporating spray turbulent dispersion: Eulerian model and numerical simulation. PhD thesis, Ecole Centrale Paris, available at <http://tel.archives-ouvertes.fr/tel-00443982/en/>.
- DOISNEAU, F., DUPAYS, J., MURRONE, A., LAURENT, F. & MASSOT, M. 2012a Eulerian VS Lagrangian simulation of unsteady two-way coupled coalescing two-phase flows in solid propellant combustion. Forthcoming in *C. R. Mec. Acad. Sc.*
- DOISNEAU, F., LAURENT, F., MURRONE, A., DUPAYS, J. & MASSOT, M. 2012b Eulerian Multi-Fluid models for the simulation of dynamics and coalescence of particles in solid propellant combustion. Forthcoming in *J. Comp. Physics*.
- DOISNEAU, F., SIBRA, A., DUPAYS, J., MURRONE, A., LAURENT, F. & MASSOT, M. 2012c Numerical strategy for two-way coupling in unsteady polydisperse moderately dense sprays. Submitted to *J. Prop. Power*.
- DUKOWICZ, J. K. 1980 A particle-fluid numerical model for liquid sprays. *J. Comput. Phys.* **35** (2), 229–253.
- FOX, R. O., LAURENT, F. & MASSOT, M. 2008 Numerical simulation of spray coalescence in an Eulerian framework: Direct (Q)uadrature Method Of Moments and Multi-Fluid method. *J. Comput. Phys.* **227** (6), 2215–2222.
- HYLKEMA, J. J. & VILLEDIEU, P. 1998 A random particle method to simulate coalescence phenomena in dense liquid sprays. In *Proc. 16th Int. Conf. on Num. Meth. in Fluid Dyn.*, **515**, 488–493. Arcachon, France.
- KAH, D., LAURENT, F., FRÉRET, L., DE CHAISEMARTIN, S., FOX, R., REVEILLON, J. & MASSOT, M. 2010 Eulerian quadrature-based moment models for dilute polydisperse evaporating sprays. *Flow Turbulence and Combustion* **85** (3–4), 649–676.
- LAURENT, F. & MASSOT, M. 2001 Multi-fluid modeling of laminar poly-dispersed spray flames: origin, assumptions and comparison of the sectional and sampling methods. *Comb. Theory and Modelling* **5**, 537–572.
- LAURENT, F., MASSOT, M. & VILLEDIEU, P. 2004 Eulerian Multi-Fluid modeling for the numerical simulation of coalescence in polydisperse dense liquid sprays. *J. Comp. Phys.* **194**, 505–543.
- LEVERMORE, C. & MOROKOFF, W. 1998 The Gaussian moment closure for gas dynamics. *SIAM J. Appl. Math.* **59** (1), 72–96.
- REVEILLON, J. & DEMOULIN, F. X. 2007 Effects of the preferential segregation of droplets on evaporation and turbulent mixing. *J. Fluid Mech.* **583**, 273–302.
- THOMINE, O. 2011 Développement de méthodes multi-échelles pour la simulation numérique des écoulements réactifs diphasiques. PhD thesis, Université de Rouen.
- VIÉ, A., DOISNEAU, F., LAURENT, F. & MASSOT, M. 2012a On the Anisotropic Gaussian closure for the prediction of inertial-particle laden flows. Submitted to *Comm. in Comp. Physics*.
- VIÉ, A., MASI, E., SIMONIN, O. & MASSOT, M. 2012b On the direct numerical simulation of moderate-Stokes-number turbulent particulate flows using algebraic-closure-based and kinetic-based moment methods. *Proceedings of the Summer Program 2012, Center for Turbulence Research, Stanford University*, 1–10.
- WILLIAMS, F. A. 1958 Spray combustion and atomization. *Phys. Fluids* **1**, 541–545.